UNIVERSITY OF
BATH

University of Bath

Alternative formats
If you require this document in an alternative format, please contact:
openaccess@bath.ac.uk

Spectral and time domain characteristics of single muscle fibre action potentials during continuous activity extracted from model considerations

N. Radicheva, G. Slavcheva

Institute of Biophysics, Bulgarian Academy of Sciences, Acad. G. Bontchev St. bl. 21, 1113 Sofia, Bulgaria

Abstract. A model of the muscle fibre extracellular action potentials (ECAPs) calculation using experimentally recorded intracellular action potentials (ICAPs) has been applied to investigate the effect of repetitive stimulation on the electrical activity of isolated frog muscle fibres. The ECAPs were calculated both at small (0.01 mm) and at large (5 mm) radial distances to the fibre axis, and their relationship with the original ICAP parameters has been inferred. Fourier transformation of the calculated ECAPs in order to obtain the spectral characteristics and to trace out their behaviour during continuous fibre activity was performed. Stimulation frequency dependence on the ECAP time characteristics and on the shift of the maximum spectral density towards low frequencies at small and large radial distance were observed. The spectral density peak frequency is propagation velocity (PV)-dependent. The advantage of the presented method over the available experimental extracellular recording techniques from isolated muscle fibers is the possibility to show the effect of continuous muscle fibre activity on the parameters of the ECAPs and their spectral characteristics at large radial distance, which is not experimentally accessible. Our results are in agreement with those experimentally obtained. The results from the model prove the role of changes in PV of excitation along the muscle fibres (representing the last link in the complex organized motor system) in the development of fatigue.

1 Introduction

The following sequence of events form the three main links (units) of the complex organized motor system: central command with activation of α-motoneurones (i), conduction of the excitation down to the neuromuscular

junction (ii), and depolarization of the surface muscle fibre membrane, initiation and propagation of the action potential into the transversal tubules and to the fibre ends (iii), Skeletal muscles as "motors" which are able to convert chemical energy into mechanical work have a serious weakness: their performance deteriorates with prolonged activity, resulting in a decreased power output. Thus, in most cases fatigue, defined usually as an inability to maintain or regenerate the original force, is localised in the muscle itself. The slowing of the relaxation as a feature of muscle fatigue results in a reduction of activation frequency without any appreciable loss of force (Jones 1981; Mannion and Dolan 1996). The fatigue-related decline in the action potential amplitude leads to incomplete activity and loss of force (Fuglevand 1995). Intra- and extracellular recordings of single muscle fibres have shown the sarcolemmal action potential amplitude decrease and an increase of the time parameters during prolonged activity (Metzger and Fitts 1986; Radicheva et al. 1986; Balog et al. 1994) and their stimulation frequency and fibre stretch dependence (Radicheva et al. 1986, 1994; Mileva and Radicheva 1996).

Electromyographical (EMG) power spectral statistics are extensively used to monitor muscle fatigue. The power spectral density of the myoelectric signal undergoes frequency compression during fatigue (Lindström et al. 1970; Stulen and De Luca 1981). The distribution of spectral power between the different frequencies of the EMG power spectrum obtained from the whole muscle corresponds to the frequency distribution of the power in the action potentials of the individual muscle fibres of which it is composed. The power spectral shifts observed during fatigue could be attributed to a progressive slowing of conduction velocity, which leads to prolongation of the fibre action potential wave form (Lindström 1970; Lindström et al. 1970; Mortimer et al. 1970; Gath and Stålberg 1975).

The single fibre recording technique has permitted selective recording from single muscle fibres in humans in situ (Ekstedt 1964; Stålberg 1966). Nevertheless, experiments with isolated muscle fibres are a useful model for experimental and clinical EMG where surface-

Correspondence to: N. Radicheva
e-mail: ninar@iph.bio.bas.bg,
bg, gaby@iph.bio.bas.bg
Tel.: +359 2 979 2103 Fax: +359 2 971 2493

recorded potentials are usually interpreted. The registration of the extracellular potential field of active isolated muscle fibre is limited to 3 mm from the fibre axis (Gydikov et al. 1986a). Due to the low potential amplitude and unfavourable signal-to-noise ratio, there are no experimental data available at larger radial distances at which motor unit (MU) potentials are registered by means of the surface EMG methods. These data are of interest since the shape of the MU action potential is similar to that of the single muscle fibre extracellular potential at large radial distances (Gydikov 1992). Therefore, it is worth performing model investigations to predict the changes in different muscle fibre extracellular potential characteristics at large radial distance from the fibre axis during the long-lasting activity.

The present study aims to verify the applicability of a previously described model for numerical calculation of muscle fibre extracellular action potentials (ECAPs; Slavcheva et al. 1996) to the experimental set-up when the ICAPs have been recorded during continuous activity elicited by repetitive stimulation with different frequencies of the stimulus pulses. To do this, we studied (i) the dependence of the calculated ECAP parameters on the parameters of the experimentally recorded intracellular action potentials (ICAPs) during continuous activity; (ii) the time and spectral characteristics of the ECAPs both at small and large radial distances; (iii) the time and spectral characteristics of ECAPs depending on the stimulation frequency.

2 Materials and methods

Bundles of frog muscle fibres isolated from the gastrocnemius muscle as previously described (Gydikov et al. 1986b) were extracellularly stimulated with three stimulation frequencies: $f_1 = 5$ Hz, i.e. interstimulus interval (ISI) = 200 ms, $f_2 = 6.7$ Hz, ISI = 150 ms, and $f_3 = 10$ Hz, ISI = 100 ms, during 3-min trials (series). The pauses between the trials lasted 2 or 3 times longer than the trial itself in order to achieve complete recovery, estimated by the potential parameters and the propagation velocity of the excitation at the beginning of the trial.

The ICAPs were recorded by conventional microelectrode technique. The position of the electrode during recording was located by ocular micrometer scale-net of a travelling microscope between two markers. The distance between them (the poles of the stimulating electrode and microelectrode tip) was measured in mm and referred to further as d. It was used for propagation velocity (PV) calculation. The ICAPs recorded during the trials were stored on video tapes and were sampled at 25 kHz by a 12-bit analog-to-digital CED 1401 (Cambridge Electronic Design). The program Spike2 was used for data acquisition. A program was developed in its environment for extracting definite potential from the series at an arbitrary time moment of the record and for determination of its amplitude and time parameters (summarized in Table 1). The calculation of the ECAPs from the experimentally recorded ICAPs was performed in accordance with the model and its numerical implementation as described in Slavcheva et al. (1996). A program for determining the ECAP parameters (summarized in Table 2) has been developed. The spectral analysis is performed using standard single series Fourier analysis program with Hamming smoothing data window.

Six ICAPs from each of the three series (with stimulation frequencies f_1, f_2 and f_3) were selected for analysis. Due to the differing duration of the continuous activity according to the stimulation frequencies, the ICAPs were extracted from the records at equi-distant time intervals as follows: 30 s at ISI = 200 ms, 10 s at ISI = 150 ms and 5 s at ISI=100 ms.

The parameters of the ICAPs and ECAPs considered are shown in Fig. 1. In order to estimate the changes in the ICAP parameters induced by the repetitive stimulation, we have introduced a uniform time window within which all potentials in the set have been restricted. The width of this time window has been defined for the first ICAP in the series as the time interval w between the onset of the potential and the first minimum of its repolarization phase. Thus, the results reflected the parameter alterations at equal potential duration during the determined time interval.

We have adopted the PV definition as a ratio between the distance d, defined above, and the time interval C_t, measured from the end of the stimulus artifact to the maximum ICAP depolarization ($PV = d/C_t$) (Bigland-Ritchie et al. 1981), which means that the velocity of membrane depolarization processes is incorporated.

3 Modelling and computational considerations

The computational method employed for calculating the time dependence of the extracellular potential at a given
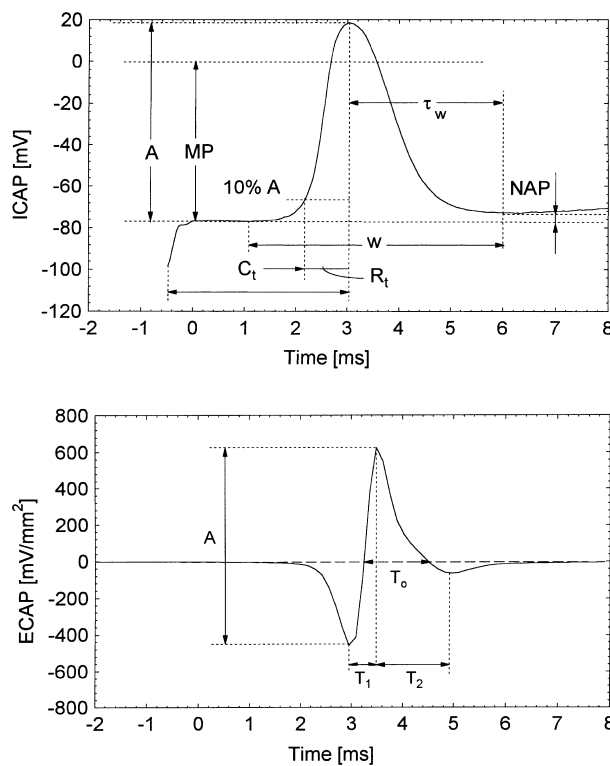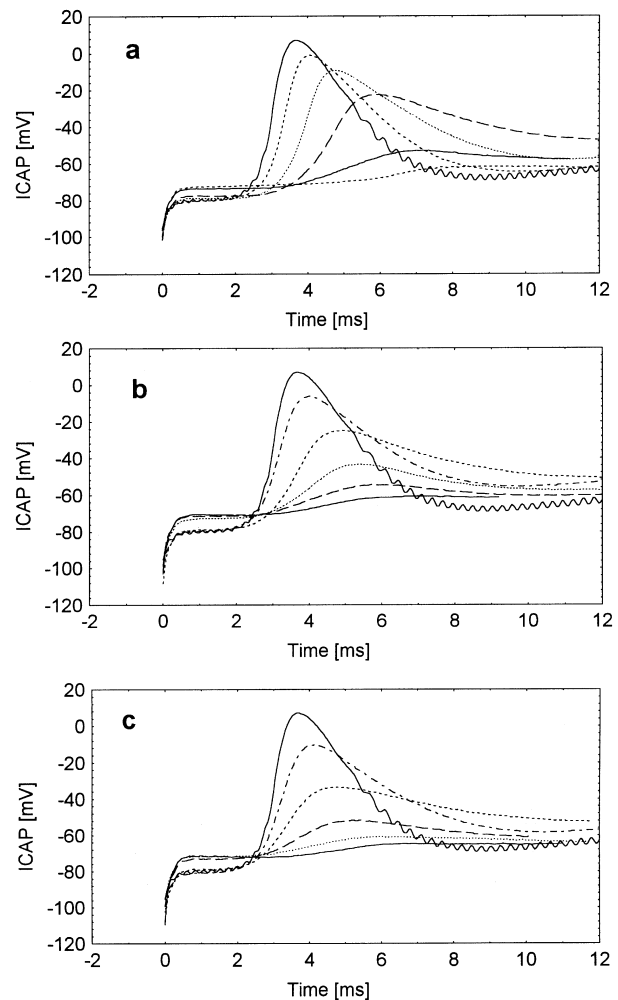

Fig. 1. Experimentally recorded ICAP and calculated ECAP with their parameters. ICAP: A, amplitude; MP, membrane potential; Rt, rising time; time interval between the peak in the depolarization phase and the potential rise at a level $10\% A$; w, time window defined for the first ICAP in the series as the time interval between the onset of the potential and the first minimum of its repolarization phase; τ_w time interval between the maximum in the depolarization phase and the end of w; C_t, the so-called conduction time of the excitation; NAP, negative afterpotential measured as the amplitude between the first minimum of the repolarization phase and the base line. ECAP: time interval between the positive and negative maximum (T_1), time interval between the interception points of the negative phase with the baseline, i.e. the negative ECAP's phase duration (T_0), and time interval between the maximum of the negative phase and the peak of the second positive phase (T_2)

point follows the procedure described in our previous work (Slavcheva et al. 1996). The basic concept used to interrelate the extracellular to the experimentally registered intracellular potential is the line-source model implemented to a semi-infinite cylindrical fibre with a conical end immersed in an isotropic and homogeneous volume conductor (Plonsey 1974). The conical taper model of the fibre end was proposed in Trayanova (1983). The main assumptions of the model implemented in the present work (as well as in the previous one) are of a propagation velocity which is proportional to the fibre radius (experimentally confirmed by Håkanssón 1956) and of a quasistationary propagation mode of the ICAP along the fibre, i.e. the PV at a point of the cone at a certain radius is equal to the PV along the cylindrical fibre with the same radius. These assumptions lead to a relation between the co-ordinates of the ICAP along the fibre with respect to the moving co-ordinate system (attached to the ICAP) and the resting co-ordinate system with an origin at the apex of the cone [see (6), Slavcheva et al. 1996] which in turn modifies the argument of the ICAP and the co-ordinate-dependent weighting function in the conical region [(5) ibid]. The assumption of a propagation velocity proportional to the fibre radius together with the conical geometry of the fibre end lead to linear dependence of the propagation velocity on the distance within the conical taper end, i.e. PV changes linearly from a value corresponding to the middle cylindrical segment of the fibre up to zero at the fibre end. The main theoretical consequence of the model is the unchanged shape of the ICAP in the time domain, even when it enters the taper. This is in agreement with the experimental data (Falck and Fatt 1964; Katz and Miledi 1965; Adrian et al. 1970; Gydikov et al. 1986b).

On the other hand, morphological studies of skeletal muscle fibres (Schwarzacher 1960) reveal gradual changes of the radius of the cylindrical part of the fibre as well as changes in the shape of ECAP when passing into a terminal part decreasing to zero (Gydikov et al. 1986b). These experimental studies allow us to claim that the above model is adequate for the object of investigation.

The model investigation of the registered signals proceeds as follows. The equidistant ICAPs are extracted from the time record during acquisition, giving a set of potentials presented in Fig. 2 at the three frequencies of stimulation. The data are fitted as a function of distance along the fibre axis within the above defined time window using the approximation function introduced in Slavcheva et al. (1996). The space distribution of each ICAP in the series is obtained using the corresponded PV during continuous activity computed according to the procedure described in the previous section. The first derivative of the space distribution of the ICAP is directly substituted in the (4), Slavcheva et al. (1996), in order to obtain the time distribution of the extracellular potential at an axial distance of $z = 17$ mm (far from the fibre end and from the site of stimulation, i.e. the artificial end plate) and two radial distances, correspondingly $r = 0.01$ mm (i.e. small

Fig. 2. Experimentally recorded ICAPs from one muscle fibre during continuous activity at equidistant time intervals of 30 s (**a**); of 10 s (**b**) and of 5 s (**c**) under stimulation with ISI = 200 ms, 150 ms and 100 ms, respectively

radial distance) and $r = 5$ mm (large radial distance) from the fibre axis.

The calculated ECAPs are further processed in order to obtain the Fourier spectra and perform spectral analysis. The spectral density is computed by smoothing the periodogram values, using the Hamming moving average window. By smoothing the periodogram it is possible to identify the general frequency regions, consisting of many adjacent frequencies (or spectral densities) that significantly contribute to the overall periodic behaviour of the series. The weights for the weighted moving average of the periodogram values are computed according to the formula:

$$w_j = 0.54 + 0.46 \cos\left(\frac{xj}{p}\right), \quad (j = 0, p)$$

$$w_{-j} = w_j \quad (j = 0)$$

where, $p = \frac{(m-1)}{2}$, m is the width of the moving average window. Choosing $m = 5$, the above expression leads to the following values of the weights: 0.0357, 0.2411,

0.4464, 0.2411, 0.0357 at which the calculations have been performed.

4 Results

The pattern of muscle fibre activity during the trials depended on the stimulation frequency and the type of the fibre. These factors determined the duration of the period of continuous activity which was followed by intermittent activity. Slow muscle fibres had a longer duration of continuous activity than fast muscle fibres (Mileva and Radicheva 1996). We studied the influence of repetitive stimulation on the continuous activity of slow muscle fibres, which was 150–180 s at stimulation with ISI = 200 ms. The ICAPs shown in Fig. 2 were extracted from uninterrupted records at equidistant time intervals of 30, 10 and 5 s, respectively, during the period of continuous activity. With increasing stimulation frequency, the time duration of continuous activity becomes shorter (it was 50 s at ISI = 150 ms and 25 s at ISI = 100 ms).

The ECAPs are calculated at an arbitrary axial position (z = 17 and 0 mm from the fibre end) which is of importance for the potential shape. In contrast, the ICAP shape does not depend on the axial distance from the fibre end (Gydikov et al. 1986b), and therefore no correspondence between the time axis of the ICAP and the ECAPs in the figures presented is required. The calculated ECAPs at small and large radial distances are shown in a three-dimensional plot (Fig. 3) as a function of its time position in the series. The decrease of the amplitude and the increase of the time duration of the ECAPs during continuous activity are clearly observed both at small and large radial distances. The shape of the sixth ECAP at small radial distances at ISI = 200 ms and ISI = 150 ms is distorted, especially the first positive phase (Fig. 3a,b, top), because of the greater increase of the ICAP latency, shift of the baseline and decrease of the ICAP amplitude. Consequently, the exact determination of the onset of the experimentally registered potential was uncertain. At large radial distances the ICAP repolarization phase contributes more to the ECAP shape and especially to the terminal positive phase (Fig. 3a,b,c, bottom), visible only at large radial distances (Dimitrov and Dimitrova 1979; Gydikov et al. 1986a; Slavcheva et al. 1996). During long-lasting activity the low amplitude and increased duration of the terminal positive phase realistically reflects the effect of the slow ICAP repolarization phase as well as its slow and small depolarization.
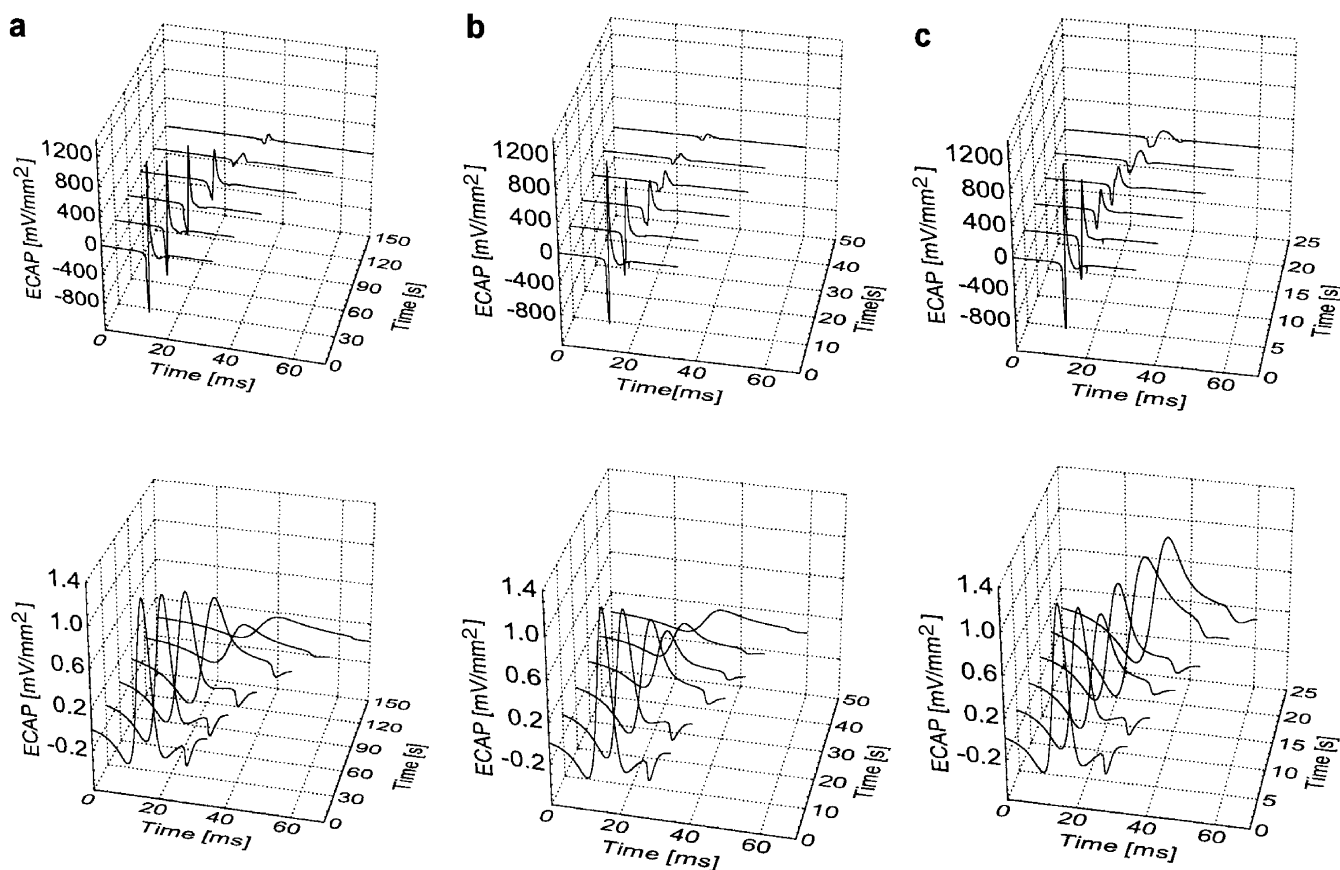
Fig. 3a–c. ECAPs calculated from the ICAPs in Fig. 2 at axial distance z = 17 mm from the fibre end and radial distances from the fibre axis: r = 0.01 mm (*top*) and r = 5 mm (*bottom*). ECAPs are presented at equidistant time intervals of 30 s upon repetitive stimulation with ISI=200 ms (**a**); 10 s time intervals upon stimulation with ISI = 150 ms (**b**); 5 s time intervals at ISI = 100 ms (**c**). The *third axis* corresponds to the time position of the potential in the series during continuous activity

Table 1. Parameters of the intracellular action potentials (ICAPs) experimentally recorded under stimulation with interstimulus interval = 200 ms at 30-s intervals, ISI = 150 ms at 10-s intervals and ISI = 100 ms at 5-s intervals

ISI = 200 ms				ISI = 150 ms				ISI = 100 ms			
Amplitude A (mV)	NAP (mV)	Rt (ms)	v (m/s)	Amplitude A (mV)	NAP (mV)	Rt (ms)	v (m/s)	Amplitude A (mV)	NAP (mV)	Rt (ms)	v (m/s)
87.76	13.68	1.24	1.223	87.76	13.68	1.24	1.223	87.76	13.68	1.24	1.223
78.74	15.72	1.4	1.106	74.59	27.62	1.68	1.106	71.95	31.09	1.80	1.085
70.44	26.72	1.72	0.950	54.81	35.71	2.36	0.913	45.64	32.33	2.24	0.966
56.05	37.76	2.48	0.777	30.01	18.06	2.60	0.846	21.53	14.29	2.56	0.871
21.22	17.95	3.52	0.646	17.46	11.90	3.00	0.793	11.64	10.83	3.44	0.767
11.22	10.49	6.28	0.542	11.35	10.90	4.36	0.646	7.98	7.43	3.12	0.689

Table 2. Time parameters of calculated extracellular action potentials (ECAPs) under stimulaction with interstimulus interval = 100 ms, 150 ms and 200 ms at small radial distances ($r = 0.01$ mm)

ISI = 200 ms			ISI = 150 ms			ISI = 100 ms		
T_0	T_1	T_2	T_0	T_1	T_2	T_0	T_1	T_2
2.005	0.520	2.993	2.005	0.520	2.993	2.005	0.520	2.993
2.115	0.612	3.576	2.418	0.849	3.489	2.023	0.815	3.980
2.711	0.747	3.522	2.830	0.995	3.372	3.601	1.400	4.901
2.996	0.950	3.292	2.669	1.963	2.830	3.539	1.911	3.823
3.010	3.497	1.711	3.712	2.679	3.490	3.600	3.527	2.238

The parameters determined from the experimentally recorded ICAPs and the ECAPs calculated at small radial distance are summarised in Tables 1 and 2, respectively. The values of the sixth ECAP parameters are not given for the reasons described above concerning mainly the first positive phase.

As can be seen from Table 1, the absolute value of NAP tends to increase (especially in the first 3–4 potentials in the set) during continuous activity, while the ICAP amplitude decreases (7.8, 7.7 and 10.9 times, respectively) with the stimulation frequency increase. The ratio NAP/A increases monotonously, and for the last potential in the series it was approximately 6 times its initial value at all the stimulation frequencies considered because of the continuous activity shortening with ISI decrease.

It could be seen that at ISI = 200 ms, 150 ms and 100 ms PV decreases, while Rt increases. The duration of τ_w, limited within the previously determined time window, decreased with an increase in Rt. It is clear that the parameters most strongly changed are the ICAP ones upon stimulation with ISI = 200 ms due to the longest duration of continuous activity (150 s) compared with that at ISI = 150 ms (50 s continuous activity) and ISI = 100 ms (25 s).

As can be seen from Table 2, the relative increase of the time parameter T_1 at all stimulation frequencies is about 5–6.7 times, which is greater than the relative increase of the other two parameters, T_0 (1.5–1.9 times) and T_2 (about 1.2 times). The second positive phase (T_2) is hardly experimentally detectable in cases when PV does not exceed 1 m/s, which could explain the decrease of the T_2 values in the last potentials. Moreover, T_2 is often absent, and the potential is biphasic (positive and negative phases).

The resulting spectral density upon the three stimulation frequencies under examination corresponding to ISI = 200 ms, 150 ms and 100 ms are shown in Fig. 4. Upon increasing the stimulation frequency, the spectral density peak at small radial distances from the fibre axis (Fig. 4a,b,c, top) shifts towards the low frequencies. At ISI = 200 ms this shift is more pronounced after the first minute of continuous activity, which is accompanied by an abrupt decrease of spectral density peak amplitude (Fig. 4a, top). At large radial distances a shift towards low frequencies and decrease of the spectral density peak is observed (Fig. 4a, bottom). A monotonous decrease of the spectral density and low-frequency shift during continuous activity is observed at small radial distances as well as at large radial distances at ISI = 150 ms. The most pronounced low-frequency displacements and non-monotonous decrease in spectral density peak amplitude both at small and large radial distances are achieved at the stimulation frequency with ISI = 100 ms.

The plot of the spectral peak frequency shift for ECAPs at a small radial distance as a function of the continuous activity, here defined as endurance time, is presented in Fig. 5. As can be seen from the slope of plots, the given maximum frequency shift is achieved more rapidly at higher stimulation frequencies (Fig. 5, 2 and 3) for a shorter endurance time.

In order to reveal more clearly the effect of the continuous activity on the ECAP spectral characteristics, the experimental intracellular potential records of four different fibres at a chosen ISI = 200 ms were processed, and the corresponding Fourier spectra of the calculated ECAPs computed and subsequently averaged at two radial distances from the fibre axis. The spectral density peak amplitude decreases both at small and large radial
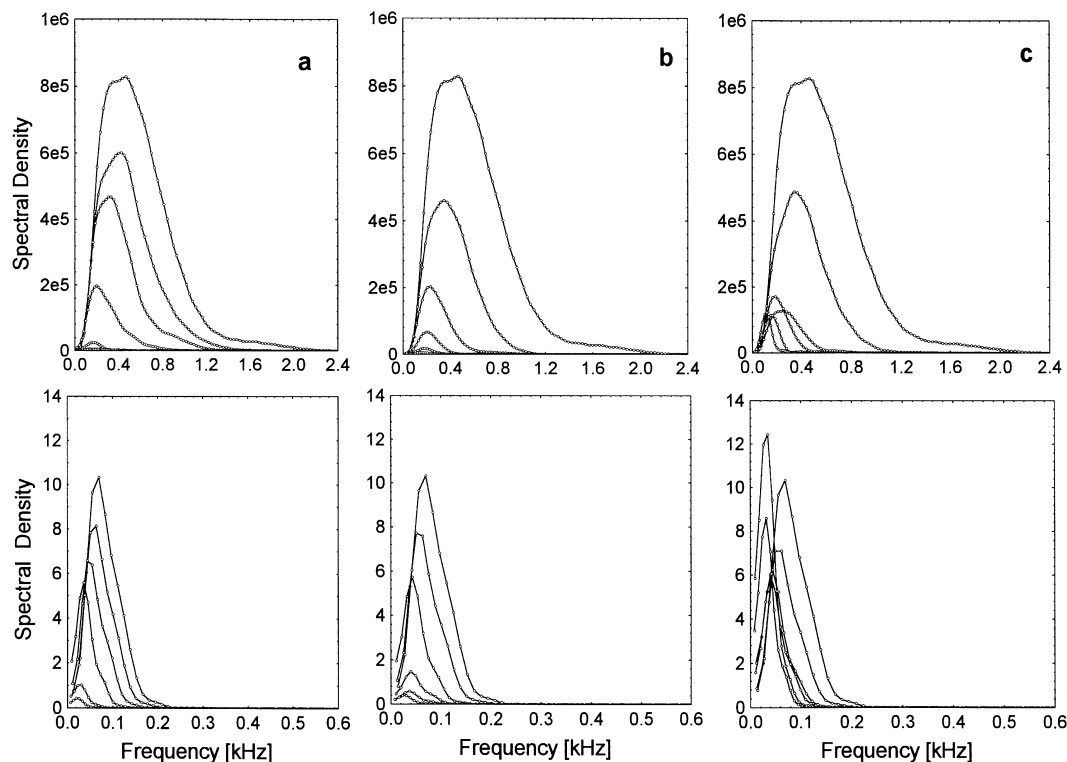
Fig. 4. Power spectrum of the calculated ECAPs at axial distance $z = 17$ mm from the fibre end and radial distances $r = 0.01$ mm (*top*) and $r = 5$ mm (*bottom*) from the fibre axis during continuous activity under repetitive stimulation with ISI $= 200$ ms (**a**), ISI $= 150$ ms (**b**) and ISI $= 100$ ms (**c**)
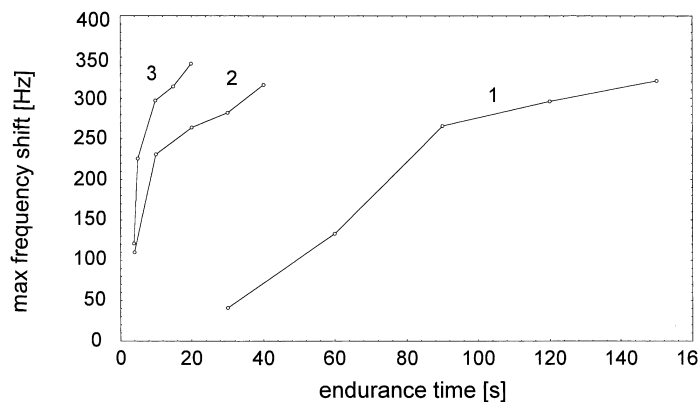

Fig. 5. Shift of the spectral peak frequency calculated for ECAP at $r = 0.01$ mm as a function of endurance time (period of continuous activity) at three stimulation frequencies: (*1*) ISI $= 200$ ms, (*2*) ISI $= 150$ ms, (*3*) ISI $= 100$ ms

distances from the fibre axis (Fig. 6a,b). The shift towards lower frequencies during long-lasting activity is monotonous, and the low-frequency shift of the spectral peak is not so abrupt and substantial compared with those at higher stimulation frequencies. The maximum frequency bandwidth is larger (~ 2.4 kHz) than that corresponding to the individual fibre bandwidth (Fig. 4a). A linear dependence between the spectral peak at small radial distances and the propagation velocity was found (Fig. 6c).

5 Discussion

The chosen experimental and model approaches turned out to be appropriate for studying the influence of

continuous activity provoked by different stimulation frequencies on the time and spectral characteristics of extracellular muscle potentials at small and large radial distances from the fibre axis. The pattern of muscle fibre activity, PV as well as the amplitude and time parameters of the ECAPs at small radial distance have been experimentally studied (Radicheva et al. 1986, 1994; Mileva and Radicheva 1996). The present results are in good agreement with these data. The ECAPs at large radial distance have a very characteristic shape, with a clearly observed terminal positive phase which during continuous activity becomes asymmetric, similar in shape to the corresponding ICAP, but with opposite sign with respect to the baseline (Dimitrov and Dimitrova 1979; Slavcheva et al. 1996). The increase of the
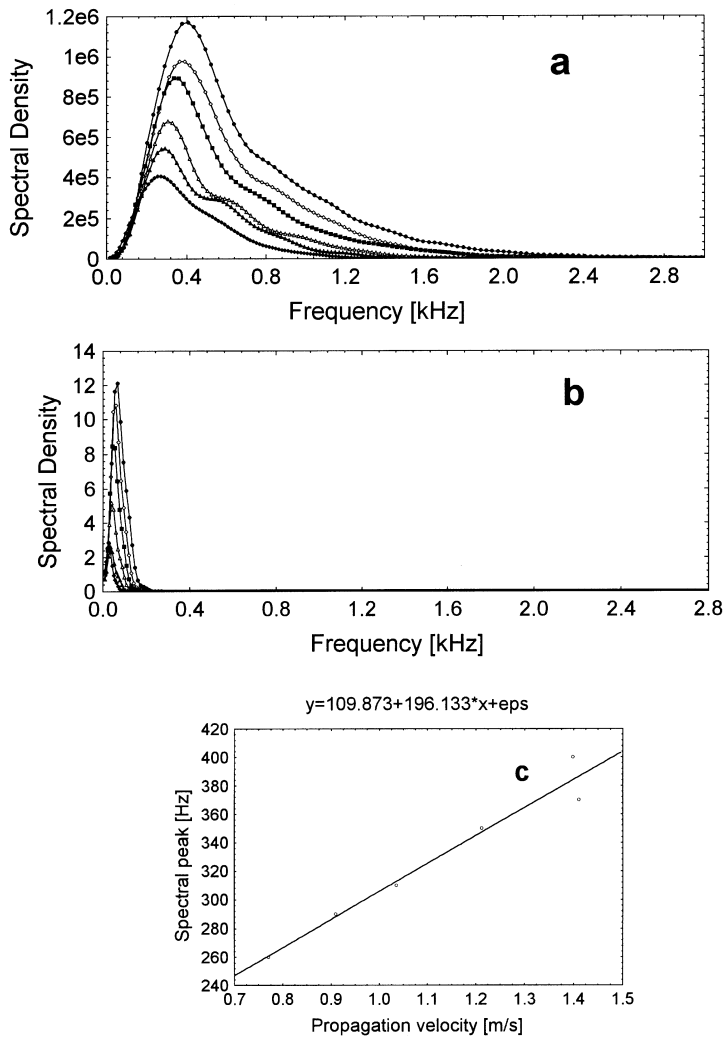
Fig. 6. Averaged spectral density plot upon stimulation frequency of 5 Hz (ISI=200 ms) at axial distance $z = 17$ mm from the fibre end and radial distance $r = 0.01$ mm (**a**) and $r = 5$ mm (**b**) from the fibre axis, and spectral peak frequency of the averaged spectral density inferred from (**a**) as a function of the propagation velocity (**c**)

latency period and the late appearance of the terminal positive phase (Fig. 3) show the PV decrease. The changes in calculated ECAPs at large distance and their relation with the corresponding experimentally obtained ICAPs during continuous activity could be used to explain the similar changes in the MU potentials studied in the contemporary EMG. As shown, the time interval T_1 at small radial distances was the parameter most greatly affected since it reflects the increased duration of the ICAP depolarization and the initial fast repolarization accompanied by PV decrease. These changes were mostly pronounced at the lowest stimulation frequency due to the prolonged period of continuous activity. With an increase of the stimulation frequency, almost the same changes were achieved for 3 to 20 times shorter continuous activity. Two aspects of the changes in the ECAP's spectral characteristics were studied: induced by long-lasting activity and as a function of stimulation frequency. The low-frequency compression of the power density spectrum in the presence of fatigue is a well-documented phenomenon (Lindström 1970; Lindström et al. 1970; Stulen and De Luca 1981; Merletti et al. 1990). The spectral shifts are mainly due to the slowing in the muscle fiber PV. According to some authors the

relationship between the reduction of the frequency and PV is proportional (Lindström 1970; Gath and Stålberg 1975; Arendt-Nielsen and Mills 1988). Our results confirm these findings. In addition, they reveal that with an increase of stimulation frequency, the shift to the lower frequencies is more pronounced and time-dependent (shown in Fig. 5, where the duration of continuous activity is called endurance time). At large radial distances the compression of the power spectrum towards low frequencies is more strongly expressed, probably due to the stronger effect of PV on ECAP parameters (Dimitrov and Dimitrova 1996). The demonstrated linear dependence between PV and spectral density peak at small radial distances remains valid also at large radial distances. The increase of stimulation frequency implies a non-monotonous decrease in spectral density peak and a low-frequency shift. Fatigue in skeletal muscle is associated with characteristic changes in the power spectrum, namely increased low-frequency activity and high-frequency decay. The spectral characteristics are related to ECAP changes induced during continuous activity, which is proof that the spectral shift primarily reflects peripheral intrinsic muscle properties (Mills 1982; Kranz et al. 1983). Access to physiological

data within the muscle shows time-dependent changes of processes related to sodium and potassium ion concentration shifts during high-frequency-induced continuous activity. They affect the muscle fiber membrane properties, the parameters of muscle fiber action potential and, in turn, the myoelectric signal leading to myoelectric muscle fatigue that is distinct from the mechanical one. Thus, the last, effectory link (muscle fibre) in a highly organized motor system very often becomes the principal locus for fatigue development and may regulate the motoneurone firing rate according to the so-called sensory fatigue hypothesis (Bigland-Ritchie et al. 1986).

6 Conclusions

This model study of the ECAP parameters based on the analytical function approximating the experimentally recorded ICAP during continuous activity is an appropriate approach for investigation of the induced changes in potential parameters. The model describes correctly the ECAPs and their spectral characteristics both at small and large radial distances from isolated, repetitively stimulated muscle fibers, which is evident from the good correspondence of the model results with experimentally obtained data. The resulting changes in the ECAP parameters and their spectral characteristics at large radial distances could be used for precise evaluation of MU potentials recorded under the same conditions of the EMG investigations. The stimulation frequency-dependent changes in muscle fibre membrane properties lead to a change in PV, which determines the time and spectral characteristics of bioelectrical muscle activity. Muscle fatigue causes changes, considered as the possible mechanism underlying the control of processes at a higher level. In isolated muscle fibre, where no restrictions are imposed by the central nervous system, the failure of activation is a perfect mechanism of regulation preventing the cell from damage during long-lasting activity.

References

Adrian RH, Chandler WK, Hodgkin (1970) Voltage clamp experiments in striated muscle fibres. J Physiol 208:607–644

Arendt-Nielsen L, Mills KR (1988) Muscle fibre conduction velocity, mean power frequency, mean EMG voltage and force during submaximal fatiguing contractions of human quadriceps. Eur J Appl Physiol 58:20–25

Balog EM, Thompson LV, Fitts RH (1994) Role of sarcolemma action potentials and excitability in muscle fatigue. J Appl Physiol 76:2157–2162

Bigland-Ritchie B, Donovan EF, Roussos CS (1981) Conduction velocity and EMG power spectrum changes in fatigue of sustained maximal efforts. J Appl Physiol 51:1300–1305

Bigland-Ritchie BR, Dawson NJ, Johansson RS, Lippold OCJ (1986) Reflex origin for the slowing motoneurone firing rates in fatigue of human voluntary contactions. J Physiol 379:451–459

Dimitrov GV, Dimitrova NA (1979) Influence of the afterpotentials on the shape magnitude of the extracellular potentials generated under activation of excitable fibres. Electromyogr Clin Neurophysiol 19:249–267

Dimitrov GV, Dimitrova NA (1996) Factor determining the M-wave spectral compression during fatigue. In: Gantchev GN, Gurfinkel VS, Stuart D, Wiesendanger M (eds) Motor Control Symposium VIII, Borovetz, Bulgaria, pp 236–240

Ekstedt J (1964) Human single muscle fibre action potentials. Acta Physiol Scand 61 [Suppl. 226]:1–96

Falck G, Fatt P (1964) Linear electrical properties of striated muscle fibres observed with intracellular electrodes. Proc R Lond Soc [Biol] 160:69–123

Fuglevand AJ (1995) The role of the sarcolemma action potential in fatigue. In: Gandevia SC et al (eds) Fatigue. Plenum Press, New York, pp 101–108

Gath I, Stålberg E (1975) Frequency and time domain characteristics of single muscle fibre action potentials. Electroencephalogr Clin Neurophysiol 39:371–376

Gydikov A (1992) Biophysics of the skeletal muscle extracellular potentials. Kluwer Academic, Dordrecht

Gydikov A, Gerilovsky L, Radicheva N (1986a) Extracellular potential field of excited isolated frog muscle fibres immersed in a volume conductor. Gen Physiol Biophys 5:125–134

Gydikov A, Gerilovsky L, Radicheva N, Trayanova N (1986b) Influence of the muscle fibre end geometry on the extracellular potentials. Biol Cybern 54:1–8

Håkanssón CH (1956) Conduction velocity and amplitude of the action potential as related to the circumference of the isolated fibre of frog muscle. Acta Physiol Scand 37:14–34

Jones DA (1981) Muscle fatigue due to changes beyond the neuromuscular junction. In: Porter R, Whelan J (eds) Human muscle fatigue: physiological mechanisms. (Ciba Foundation symposium 82) Pitman Medical, London, pp 178–196

Katz B, Miledi R (1965) Propagation of electric activity in motor nerve terminals. Proc R Soc Lond [Biol] 161:453–482

Kranz H, Williams AM, Cassel J, Caddy DJ, Silberstein RB (1983) Factor determining the frequency content of the electromyogram. J Appl Physiol 55:392–399

Lindström L (1970) On the frequency spectrum of EMG signals. Thesis, Chalmers University of Technology, Res. Lab. Med. Elect., Göteborg, Sweden

Lindström L, Magnusson R, Petersén I (1970) Muscular fatigue and action potential conduction velocity changes studied with frequency analysis of EMG signals. Electromyography 10:341–356

Mannion AF, Dolan P (1996) Relationship between myoelectric and mechanical manifestations of fatigue in the quadriceps femoris muscle group. Eur J Appl Physiol 74:411–419

Merletti R, Knaflitz M, De Luca CJ (1990) Myoelectric manifestations of fatigue in voluntary and electrically elicited contractions. J Appl Physiol 69:1810–1820

Metzger JM, Fitts RH (1986) Fatigue from high- and low-frequency muscle stimulation: role of sarcolemma action potentials. Exp Neurol 93:320–333

Mileva K, Radicheva N (1996) Stimulation frequency- and length-dependent time characteristics of muscle fibre continuous activity. In: Gantchev GN, Gurfinkel VS, Stuart D, Wiesendanger M (eds) Motor Control Symposium VIII, Borovetz, Bulgaria, pp 207–211

Mills K (1982) Power spectral analysis of electromyogram and compound muscle action potential during muscle fatigue and recovery. J Physiol 326:401–409

Mortimer JT, Magnusson R, Petersén I (1970) Conduction velocity in ischemic muscle, effect on EMG frequency spectrum. Am J Physiol 219:1324–1329

Plonsey R (1974) The active fibre in a volume conductor. IEEE Trans Biomed Eng 21:371–381

Radicheva N, Gerilovsky L, Gydikov A (1986) Changes in the muscle fibre extracellular action potentials at long-lasting (fatiguing) activity. Eur J Appl Physiol 55:545–552

Radicheva N, Vydevska M, Mileva K (1994) Stimulation frequency rate- and stretch-dependent changes in the electrical activity of slow and fast muscle fibres. C R Acad Bulg Sci 47:89–92

Schwarzacher HG (1960) Untersuchungen über die Skelettmuskel-Sehnenverbindung. III. Die Form der Muskelfaserenden. Acta Anat 43:144–157

Slavcheva G, Kolev V, Radicheva N (1996) Extracellular action potentials of skeletal muscle fibre affected by 4-aminopyridine: a model study. Biol Cybern 74:235–241

Stålberg E (1966) Propagation velocity in human muscle fibres in situ. Acta Physiol Scand 70 [Suppl 287]:1–112

Stulen F, De Luca (1981) Frequency parameters of the myoelectric signal as a measure of conduction velocity. IEEE Trans Biomed Eng 28:515–523

Trayanova N (1983) Influence of the changes in the velocity of spreading of the action potential on the distribution of the level of depolarization along an excitable fibre. Electromyogr Clin Neurophysiol 23:617